Supporting Information

Caterpillar Locomotion–inspired Valveless Pneumatic Micropump using Single Teardrop-shaped Elastomeric Membrane

Hongyun So[a], Albert P. Pisano[a], and Young Ho Seo[b,*]

[a]Department of Mechanical Engineering, Berkeley Sensor & Actuator Center, University of California, Berkeley, CA 94720, USA

[b]Department of Mechatronics Engineering, Kangwon National University, 1 Kangwon-daehak-gil, Chuncheon 200-701, Republic of Korea

[*]Corresponding Author: mems@kangwon.ac.kr

Theoretical Model

To design a simple teardrop-shaped membrane, two circles with radii of 2 mm and 0.5 mm, were connected by tangent lines. The two circles were spaced as much as 5 mm apart, from center to center. The shape of the chamber underneath the teardrop-shaped membrane was also the same as that of the membrane. The thickness of the membrane and the height of the chamber were 20 μm and 200 μm, respectively. For the theoretical estimation of the teardrop-shaped membrane, the simplified model based on the consecutive circular membranes with different radius was suggested as shown in **Fig.S1A**. Typical analytic relationship between the static pressure and deflection for a circular membrane with the radius (r), thickness (t), elastic modulus (E), and Poisson's ratio (ν) is given by

$$P = \left(\frac{Et^4}{r^4}\right)\left[k_1\left(\frac{\delta_{max}}{t}\right) + k_2\left(\frac{\delta_{max}}{t}\right)^3\right] \qquad (1)$$

where P is the applied pneumatic pressure and δ_{max} is the maximum deflection of the membrane.[38] For the membrane with a fixed edge, $k_1 = 5.33/(1-\nu)$ and $k_2 = 2.6/(1-\nu^2)$.[38] In the estimation of the membrane deflection, elastic modulus (E) and thickness of the membrane (t) was considered as 1.8 MPa[39] and 20 μm, respectively. **Figure S1B** shows the membrane deflection, which was calculated using Eq.(1), of each circular shape at the center in response to the different applying pneumatic pressure. For the same pneumatic pressure, the center deflection of the circular membrane was decreased as the radius decreased. As a result, the touchdown motion of the consecutive circular membrane was propagated from the large circular membrane to the small circular membrane. Through this simplified model based on the combination of the consecutive circular membranes, the sequent propagation of touchdown motion from the large circular membrane to the small one could be verified in the teardrop-shaped membrane.

Materials and Methods

Fabrication. The CLiMP consisted of three PDMS layers, including a teardrop-shaped chamber for fluid, a membrane for generating caterpillar-like motion, and an upper chamber for applying pneumatic pressure. Molds for the teardrop-shaped and upper chamber were made of SU-8 photoresist (MicroChem, Newton, MA), and the PDMS membrane was prepared using a spin coating process. For the upper (**Fig.S2A**) and teardrop-shaped chambers (**Fig.S2C**), the negative photoresist of SU-8 2150 was spin-coated at 2000 rpm for 30 sec onto a silicon wafer to obtain 150 μm thickness. After a soft bake at 95 °C for 30 min, patterns were defined via a contact aligner (MA6, Karl Suss) with intensity of 15.2 mW/cm^2 for 35 sec. Photoresist was developed in 1-Methoxy-2-propanol acetate for 20 min, and then baked at 90 °C for 15 min. PDMS (Sylgard-184, Dow Corning, NY) with mixing ratio of 10:1 (base : curing agent) was

casted on the patterned photoresist mold. After curing PDMS at 120 °C for 2 hours, the PDMS was separated from the photoresist mold. Inlet and outlet ports for the catheter couples (Instech Laboratories, Plymouth Meeting, PA) were punched. The thin PDMS membrane (**Fig.S2B**) between two chambers was prepared using a spin coating process. Before coating PDMS on the flat glass (Fisher Scientific, PA), the glass surface was treated with Trichlorosilane [$CF_3(CF_2)_5CH_2CH_2SiCl_3$, 97%, Sigma Aldrich] as an anti-adhesion layer in a vacuum desiccator. PDMS (10 : 1) was coated on the glass with 4000 rpm for 1 min to deposit a thickness of 20 μm. All PDMS parts were treated by oxygen plasma (RIE, PETS Inc., CA) with 20 W for 20 sec, and then bonded together at 80 °C for 2 hours. **Figures S3A** and **S3B** show SEM images of the cross section of the fabricated CLiMP and enlarged view of the PDMS membrane, respectively. The upper circular chamber for applying pneumatic pressure was not shown in **Figs.S3A** and **S3B.**

Experimental Setup. The experimental setup is shown in **Fig.S3C**. **Figure S3E** shows schematic view of the membrane deformation when the pneumatic pressure is applied. The pneumatic pressure supplied by the hydrogen gas tank was monitored using a pressure sensor (40PC500G2A, Honeywell) and controlled by a small-sized solenoid valve (225T021, Cole-Parmer). The on/off signal for the solenoid valve was controlled via a combination of a function generator (33120A, Hewlett-Packard) and voltage amplifier (PA-138, Labworks Inc.). The motion of the teardrop-shaped, bilaterally symmetric PDMS membrane was captured using a high-speed camera (Phantom Miro eX4, Vision Research), which sampled every 790 μs. The flow rate was determined by measuring the length the traveled fluid (1% methylene blue) through a 580 μm diameter tube in 5 min. The pneumatic pressure applied to the membrane,

solenoid valve control signals, motion of the membrane, and flow through the tube were recorded simultaneously.

Results and Discussion

Using the images captured by a high-speed camera, experimental results were compared with simulation results in the aspect of the touchdown (contact) area between the PDMS membrane and the bottom of the teardrop-shaped chamber. **Figure S4** presents the comparison of the contact area during the contraction period. The contact area was increased during the contraction period in both simulation and experimental results. However, the discrepancy between the estimated and experimental results was increased as the contract area was increased. Again, this implies that the viscoelastic model could be better than the elastic model for the large and fast dynamic deformation. **Figure S5** shows the measured flow rate with the different duty cycles (20, 50 and 80%) for each different pneumatic pressure (3, 4 and 5 kPa) in response to the frequencies (1–5 Hz). The number of pushing membrane per second was determined by the frequency of the pneumatic pressure, and the both propagation time of touchdown motion (contraction period, CP) and liquid refilling time (relaxation period, RP) were determined by the duty cycle. For example, for the frequency and duty cycle of 2 Hz and 20%, the number of pushing process, CP, and RP were twice a second, 0.4 sec., and 1.6 sec, respectively. Regardless of duty cycles, the flow rate generated by the CLiMP was increased as pneumatic pressure increased. However, the peak of the measured flow rate was observed at a different frequency of the applied pneumatic pressure. At a duty cycle of 20 and 50%, the maximum flow rates were measured at 1.5 and 2.5 Hz, respectively. Through the experiments, it was found that the flow rate traded off the number of pushing process, the CP and RP. As a result, at 20% duty cycle

(**Fig.S5A**), the CP was too short to propagate the touchdown motion at a frequency higher than 2 Hz, thus the maximum flow rate was measured at 1.5 Hz. On the other hand, at 50% duty cycle (**Fig.S5B**), the RP was relatively shorter than the CP to refill the liquid above 3 Hz, thus the maximum flow rate was generated at 2.5 Hz. It was also found that at 50% duty cycle, the flow rate was linearly proportional to the frequency up to 2.5 Hz where the peak value occurs, resulting in easy control of the flow rate by the combination of the frequency and amplitude of pneumatic pressure. Finally, at 80% duty cycle (**Fig.S5C**), the pumping operation was significantly limited by the RP as no flow rate was generated at the frequency higher than 2.5 Hz due to insufficient liquid refilling.

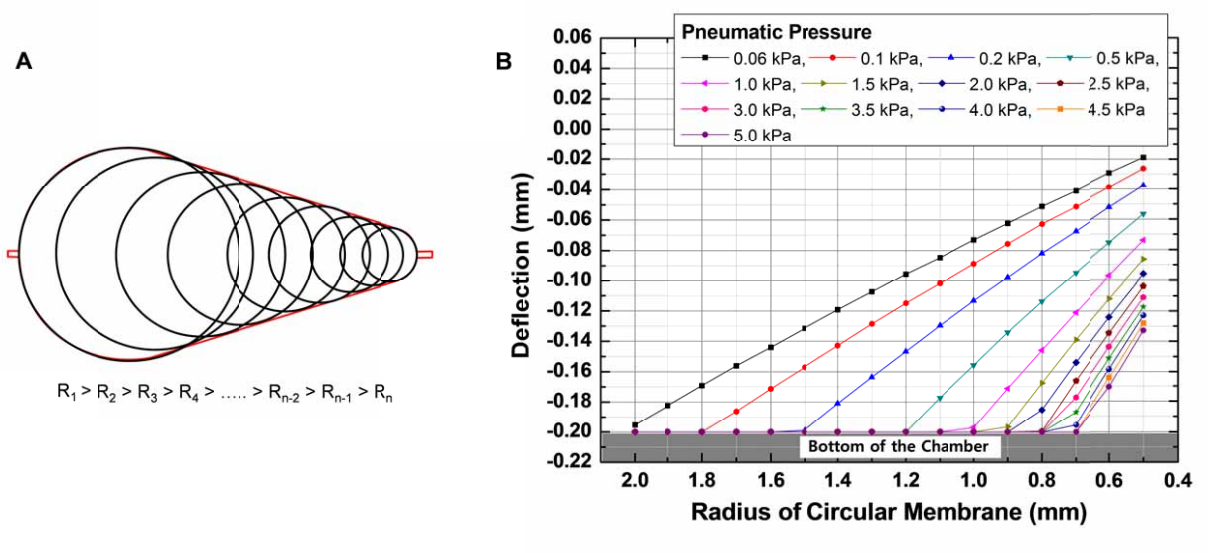

Fig. S1 Theoretical estimation of the touchdown behavior of the teardrop-shaped membrane: (A) Simplified model of the teardrop-shaped membrane based on the combination of circular membranes with different radius, (B) Membrane deflection vs radius of circular membrane for the different applied pneumatic pressure.

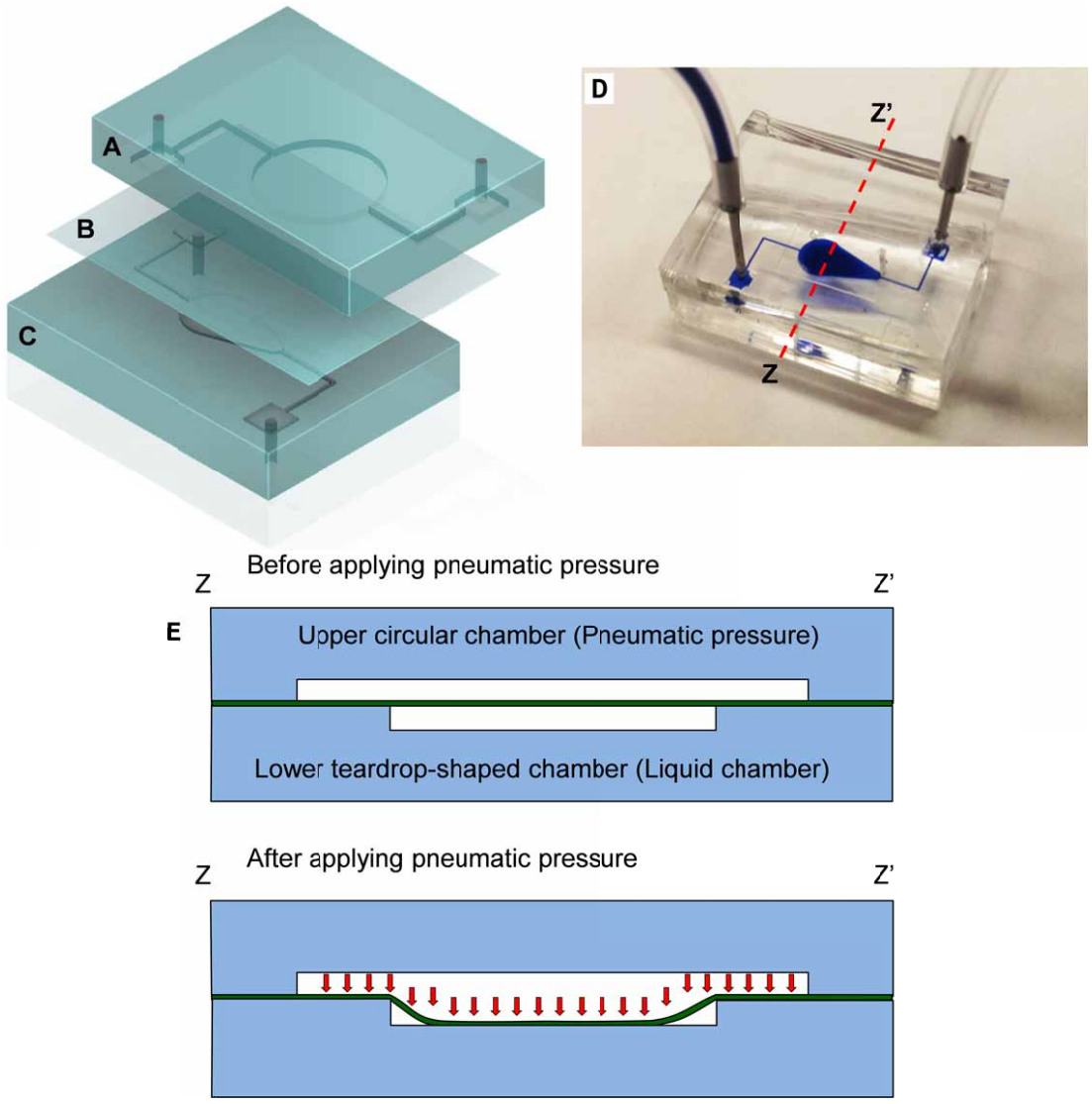

Fig. S2 Micropump fabrication using a PDMS casting process: (A) Chamber for applying pneumatic pressure, (B) PDMS membrane, (C) Teardrop-shaped chamber for transporting fluid, (D) Photograph of the fabricated caterpillar locomotion–inspired micropump, (E) Schematic view of the membrane deformation when the pneumatic pressure is applied.

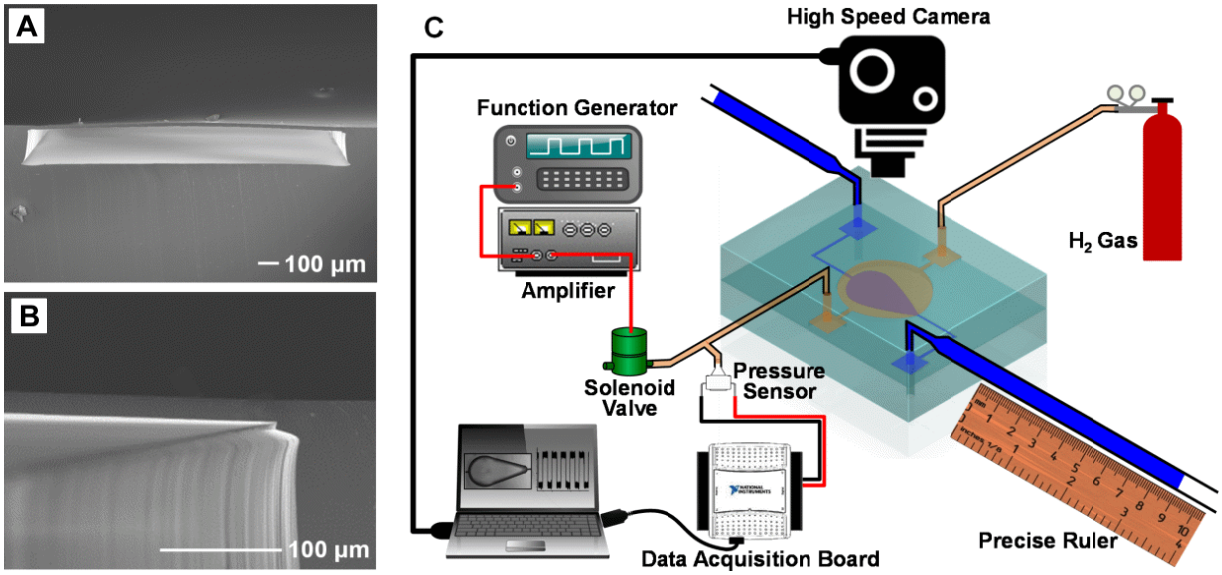

Fig. S3 Experimental method: (A) Cross-sectional SEM image of the micropump, (B) Enlarged view of PDMS membrane, (C) Schematics of experimental apparatus.

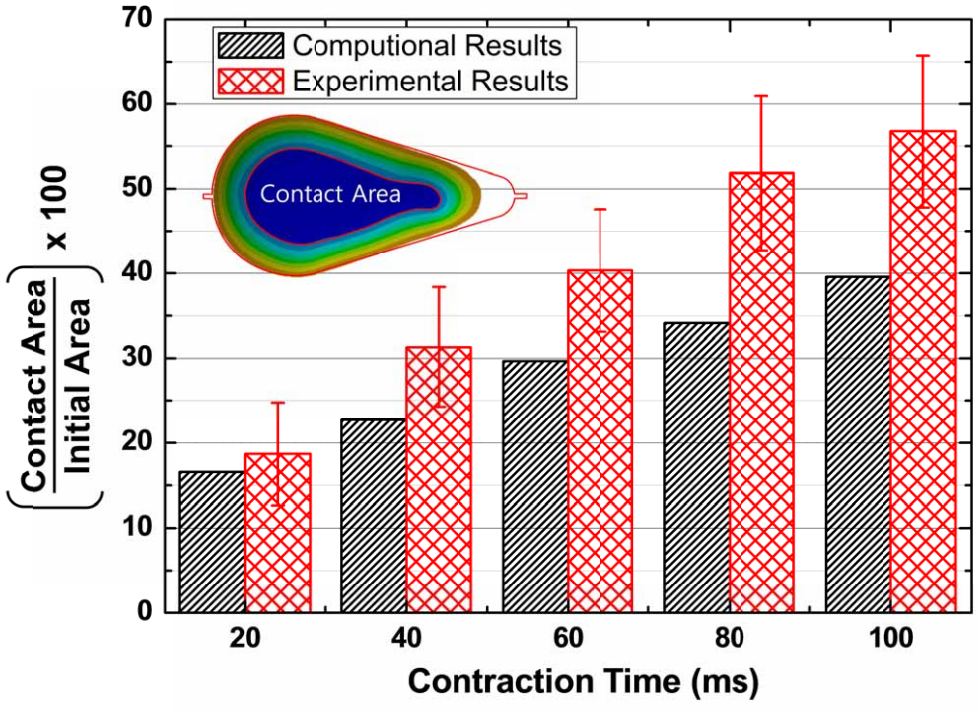

Fig. S4 Comparison between the computational and experimental results for the contact area during the contraction period.

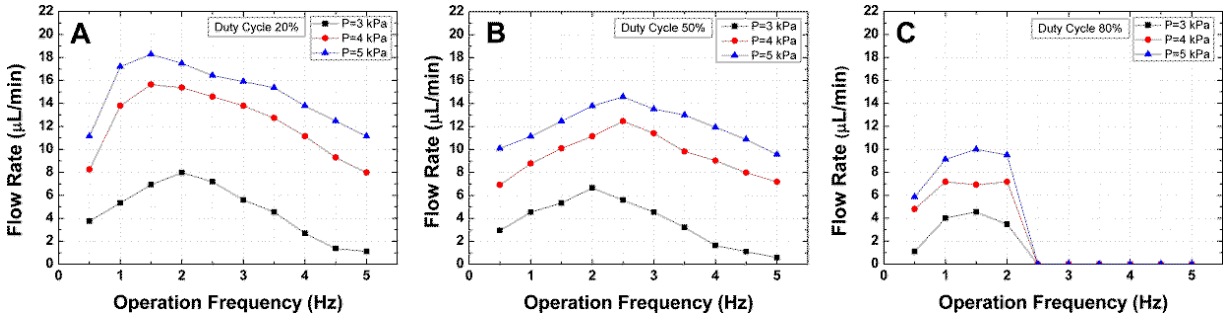

Fig. S5 Measured flow rate with respect to the frequency of applied pneumatic pressure: (A) Duty cycle of 20%, (B) 50%, (C) 80%.

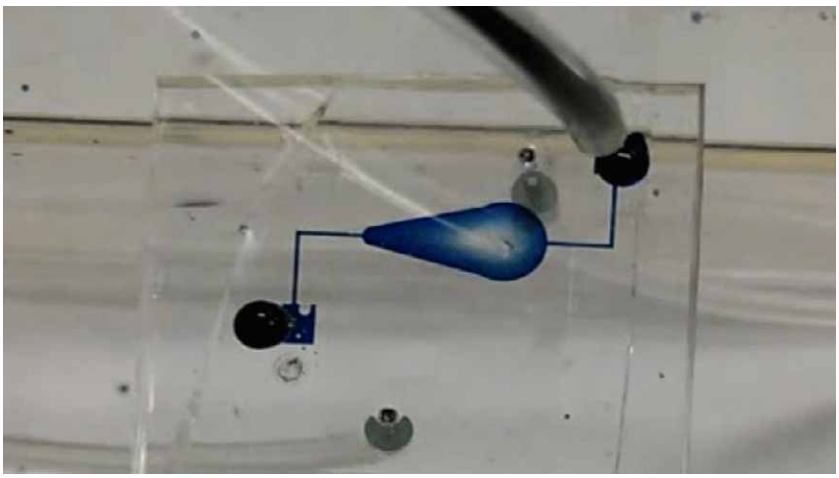

(Still-image)

Movie S1 Membrane motion of the caterpillar locomotion–inspired micropump, at a 20% duty cycle, 2 Hz frequency and pneumatic pressure of 5 kPa.

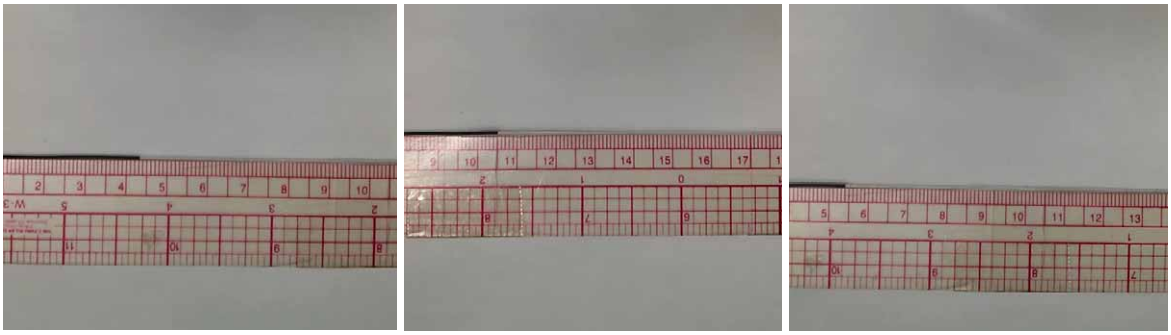

(Movie.S2A) (Movie.S2B) (Movie.S2C)

(Still-image)

Movie S2 Liquid flow through a horizontal tube without pulsating flow. Operation conditions (pneumatic pressure, frequency, duty cycle) in Movie S2A, S2B, and S2C were (5 kPa, 0.5 Hz, 30%), (5 kPa, 2.0 Hz, 30%) and (5 kPa, 4.5 Hz, 30%), respectively.

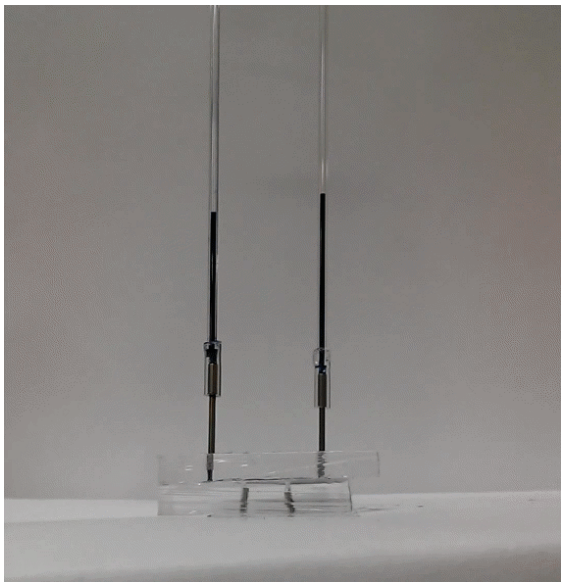

(Still-image)

Movie S3 Hydraulic head generated by the caterpillar locomotion–inspired micropump at a 20% duty cycle, 1 Hz frequency and pneumatic pressure of 5 kPa (three times faster than real speed).